
Effects of denaturants and substitutions of hydrophobic residues on backbone dynamics of denatured staphylococcal nuclease

SATOSHI OHNISHI AND DAVID SHORTLE

Department of Biological Chemistry, The Johns Hopkins University School of Medicine, Baltimore, Maryland 21205, USA

(RECEIVED February 17, 2003; FINAL REVISION April 9, 2003; ACCEPTED April 11, 2003)

Abstract

Analysis of residual dipolar couplings (RDCs) in the $\Delta 131\Delta$ fragment of staphylococcal nuclease has demonstrated that its ensemble-averaged structure is resistant to perturbations such as high concentrations of urea, low pH, and substitution of hydrophobic residues, suggesting that its residual structure is encoded by local side-chain/backbone interactions. In the present study, the effects of these same perturbations on the backbone dynamics of $\Delta 131\Delta$ were examined through ^1H - ^{15}N relaxation methods. Unlike the global structure reported by RDCs, the transverse relaxation rates R_2 were quite sensitive to denaturing conditions. At pH 5.2, $\Delta 131\Delta$ exhibits an uneven R_2 profile with several characteristic peaks involving hydrophobic chain segments. Protonation of carboxyl side chains by lowering the pH reduces the values of R_2 along the entire chain, yet these characteristic peaks remain. In contrast, high concentrations of urea or the substitution of 10 hydrophobic residues eliminates these peaks and reduces the R_2 values by a greater amount. The combination of low pH and high urea leads to further decreases in R_2 . These denaturant-induced increases in backbone mobility are also reflected in decreases in ^{15}N NOEs and in relaxation interference parameters, with the former reporting an increase in fast motions and the latter a decrease in slow motions. Comparison between the changes in chain dynamics and the corresponding changes in Stokes radius and the patterns of RDCs suggests that regional variations in backbone dynamics in denatured nuclease arise primarily from local contacts between hydrophobic side chains and local interactions involving charged carboxyl groups.

Keywords: Backbone dynamics; urea; hydrophobic interaction; NMR spin relaxation; denatured proteins

Supplemental material: See www.proteinscience.org.

In the denatured state, a polypeptide chain loses tight packing and exists as a highly dynamic ensemble of many rapidly interconverting conformations. Experimental approaches to characterization of denatured proteins invariably yield structural parameters that have undergone extensive ensemble averaging. Conventional NMR methods

provide significant information on local structures, such as turns and helices, but medium- to long-range NOEs that could provide information on long range structure are seldom detected. This laboratory has pursued structural studies of a large denatured fragment of the staphylococcal nuclease with deletion of residues at both termini, termed $\Delta 131\Delta$, for the past 10 years. Application of methods involving extrinsic spin labels and paramagnetic relaxation enhancement yielded long distance restraints that permitted calculation of conformations for $\Delta 131\Delta$ in buffer, demonstrating that this model denatured state retains a native-like low resolution structure or topology (Gillespie and Shortle 1997). Subsequent structural studies using residual dipolar

Reprint requests to: David Shortle, Department of Biological Chemistry, The Johns Hopkins University School of Medicine, Baltimore, MD 21205, USA; e-mail: dshortl1@jhmi.edu; fax: (410) 955-5759.

Abbreviations: NOE, nuclear Overhauser effect; RDC, residual dipolar coupling.

Article and publication are at <http://www.proteinscience.org/cgi/doi/10.1110/ps.0306403>.

couplings (RDCs), which provide distant-independent information on the relative orientations between individual residues (Tolman 2001; Bax 2003) have revealed that the ensemble-averaged structure of $\Delta 131\Delta$ is quite robust and persists in the presence of 8 M urea and/or upon substitution of numerous hydrophobic side chains (Shortle and Ackerman 2001; Ackerman and Shortle 2002b). These findings led us to conclude that local steric interactions, not long-range hydrophobic contacts, encode long-range structure in protein folding. We have reported observation of significant distributions in RDCs of arbitrarily selected short peptides from 2 to 15 amino acids in length, supporting this conclusion (Ohnishi and Shortle 2003).

The persistence of residual structure in the denatured state is expected to exert significant effects on the overall dynamic behavior of the polypeptide backbone. Several denatured proteins including $\Delta 131\Delta$ have been analyzed using NMR methods based on ^{15}N relaxation (Alexandrescu and Shortle 1994; Farrow et al. 1995, 1997; Schwalbe et al. 1997; Sinclair and Shortle 1999; Buevich et al. 2001; Yao et al. 2001; Schwarzinger et al. 2002). In most cases, denatured proteins exhibit profiles of relaxation containing one or more pronounced peaks, which are consistent with motional slowing or intermittent formation of structure involving a subset of amino acid residues. Through application of this NMR relaxation approach, an intriguing observation has been reported for a denatured hen lysozyme (Klein-Seetharaman et al. 2002). The lysozyme in the presence of 8 M urea at pH 2.0 exhibited an uneven profile of transverse relaxation rate (R_2) with several high values at positions in the sequence where similar peaks are observed in the native state, suggesting presence of a native-like residual structure. Surprisingly, a single mutation of W62G, which resides on the surface of the folded protein, flattened out the R_2 profile in the absence of urea, leading these authors to conclude that a network of hydrophobic clusters encodes native-like structures in the denatured protein.

This conclusion is at odds with the data for nuclease $\Delta 131\Delta$ that have led us to infer that local steric interactions encode long-range structure (Shortle and Ackerman 2001; Ackerman and Shortle 2002b). To resolve this apparent paradox, we have reexamined and extended our analysis of the dynamic properties of $\Delta 131\Delta$ (Alexandrescu and Shortle 1994). In that study, the ^1H - ^{15}N NOE, T_1 , and T_2 relaxation data of $\Delta 131\Delta$ in aqueous buffer at pH 5.2 were analyzed using a modified “model-free” formalism, which includes contributions from internal motions on both an intermediate (τ_c) and a fast time scale (τ_f) in the context of slow overall tumbling (τ_m) to obtain order parameter (S^2). The results revealed peaks in the R_2 profile, and suggested that secondary structure may be preferentially stabilized in hydrophobic segments of the chain.

In the present study, we study the effect of low pH, 8 M urea, and multiple hydrophobic to polar mutations on the

backbone dynamics of $\Delta 131\Delta$. Instead of using a set of ^1H - ^{15}N NOE, T_1 , and T_2 relaxation methods with the modified “model-free” analysis described above, we employed ^1H - ^{15}N NOE, T_2 measurements and the method of Tjandra et al. (1996), which quantitatively measures interference effects between the chemical shift anisotropy of the peptide bond and dipolar relaxation of backbone amide ^{15}N - ^1H , referred to as relaxation interference. In a previous study, this simpler method was demonstrated to give results similar to those obtained by the more conventional model free analysis (Sinclair and Shortle 1999). When the latest data are interpreted in the context of Stokes radii and RDCs analyzed under identical denaturing conditions, we conclude that local hydrophobic side-chain/side-chain contacts plus local interactions involving carboxyl groups are responsible for most, if not all, of the denatured state “structure” reported by ^{15}N relaxation data.

Results

^{15}N Relaxation profiles of $\Delta 131\Delta$

The ^1H - ^{15}N NOE, relaxation interference, and transverse R_2 profiles of $\Delta 131\Delta$ at pH 5.2, 32°C are shown in Figure 2 in solid square symbols. Although the data suggest the molecule displays much more dynamic behavior than a typical folded protein, higher values for all three parameter profiles are observed in the regions around residues 60–75 and residues 85–115, indicating that these segments of the protein chain are less flexible. Previous studies have indicated that residues 14–44, which form a three-strand beta meander in folded nuclease (Fig. 1), for a “molten” bundle of extended segments in $\Delta 131\Delta$ (Wang and Shortle 1995). This semi-stable structure displays dynamic behavior in the intermediary conformational exchange regime (μsec - msec), and thus its amide protons are not detectable by NMR.

These relaxation profiles are quite similar to those reported in a previous study (Alexandrescu and Shortle 1994), with the one exception that the present R_2 data set yielded values ~20 % smaller than previously. This difference can be attributed to viscosity effects on the correlation time; the previous study used 2.8 mM protein, while the present study used 1.2 mM.

pH effects

Lowering the pH from 5.2 to 3.0 resulted in an overall increase in dynamic motion reflected in all three relaxation profiles, while the characteristic peaks in these profiles were maintained (Fig. 2, open circles). Further reductions in the pH down to 1.2 showed no additional changes. These results suggest that interactions involving deprotonated aspartate and glutamate side chains must restrict the motional behavior of this denatured protein. Staphylococcal nuclease is rich

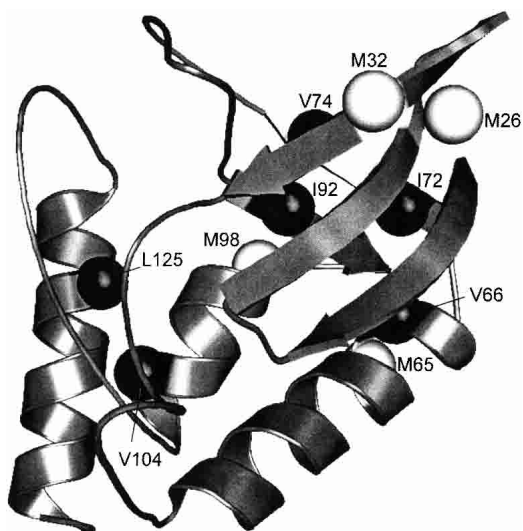


Figure 1. A ribbon diagram of staphylococcal nuclease (1SNC; Loll and Lattman 1989). The region between residue 13 and 140 is displayed. Hydrophobic residues that were replaced with hydrophilic ones in the sextuple mutant and methionines oxidized in the oxo-sextuple mutant are marked with black and white spheres, respectively, at their C_{α} position.

in charged residues (23 Lys, 5 Arg, 4 His, 12 Glu, 8 Asp), and independent evidence for residual electrostatic interaction in denatured nuclease has been presented (Whitten and Garcia-Moreno 2000). Similar pH effects on backbone dynamics have been reported for the natively unfolded form of the pro-peptide of subtilisin (Buevich et al. 2001).

Urea effects

The addition of 8 M urea at pH 5.2 reduced some of the line broadening displayed by the β -meander region, and a characteristic peak centered on residue 29 appeared in each of the relaxation profiles (Fig. 3, open triangles). This finding suggests that 8 M urea eliminates much of the β -meander structure, yet some of its motions are still constrained. The characteristic peaks observed in the absence of urea around residues 60–75 and 85–115 were drastically diminished in the R_2 profile. Although similar effects of urea are reflected in the relaxation interference profile, the NOE profile is qualitatively different. The more positive NOE values around residues 85–115 are maintained upon the addition of 8 M urea, while increased NOE values are observed in the regions around residues 40–75 and 120–140. This indicates that the fastest backbone motions (<1 nsec) in these regions are reduced. Much of this motional slowing can be attributed to the increase in solution viscosity at high concentrations of urea (1.7 cP for 8 M urea solution versus 1.0 cP for H_2O). Separate 1H - ^{15}N NOE experiments using ethylene glycol solutions with a viscosity of ~ 2.0 cP displayed very similar increases in NOE values. Although it is well known

that the slower motion of molecular tumbling is viscosity dependent, the present results show that solvent viscosity also affects fast motions on the subnanosecond time scale. Overall, the effects of urea on relaxation properties were most dramatic for the R_2 values, relatively large for relaxation interference values, and more modest on the NOEs.

The combination of both 8 M urea and pH 3.0 altered the backbone dynamics profiles even more dramatically (Fig. 3, cross signs). The characteristic peak in the β -meander region of each profile is significantly reduced and the overall profile is essentially flat. This added effect of acid pH suggests that deprotonated glutamates and aspartates still restrict fast motions in the expanded denatured state, even in 8 M urea.

Substitution of hydrophobic side chains with polar groups

To more fully reduce hydrophobic interactions in $\Delta 131\Delta$, a sextuple mutant was analyzed in which six hydrophobic residues were substituted with polar residues (V66T/I72T/V74T/I92T/V104T/L125Q) plus the four methionines (M26/M32/M65/M98) oxidized with hydrogen peroxide to

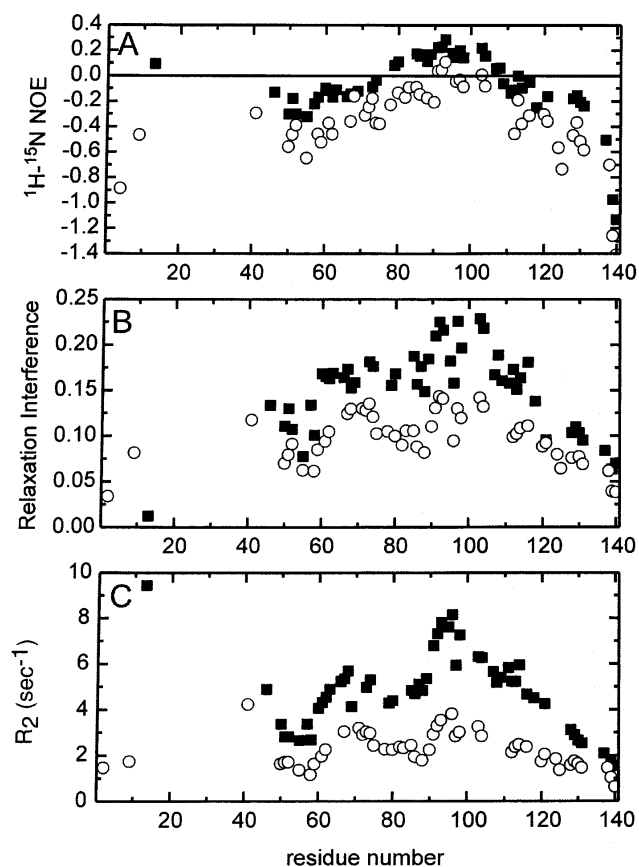


Figure 2. ^{15}N Relaxation profiles of $\Delta 131\Delta$ at pH 5.2 (squares) and pH 3.0 (circles). (A–C) ^{15}N NOE, relaxation interference, and transverse R_2 profiles, respectively.

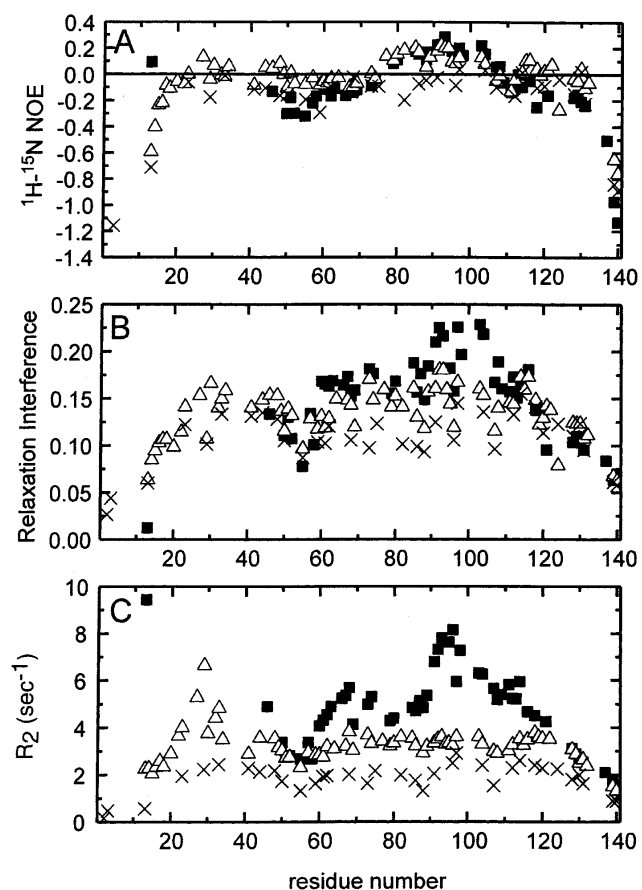


Figure 3. ^{15}N Relaxation profiles of $\Delta 131\Delta$ at pH 5.2 in the absence (solid squares) and presence (open triangles) of 8 M urea at pH 5.2. The cross signs represent data at pH 3.0 in the presence of 8 M urea. (A–C) ^{15}N NOE, relaxation interference, and transverse R_2 profiles, respectively.

the sulfoxide form (Fig. 1; Ackerman and Shortle 2002b). As shown in Figure 4 in solid triangles, the replacement of hydrophobic residues more or less eliminates the characteristic peaks around residues 60–75 and 85–115. The addition of 8 M urea did not produce further changes in the relaxation profiles, other than making residues in the β -meander region detectable and shifting the NOE profile up because of increased viscosity. The oxidization of methionines made residues in the β -meander region detectable in the absence of urea, and the overall profiles of the oxo-sextuple $\Delta 131\Delta$ were essentially flat (plus signs, left panels of Fig. 4). These results indicate that, like high concentrations of urea, substitutions of hydrophobic residues with polar groups make the molecule more dynamic by increasing fast motions. On the other hand, as described above in the introduction, our previous results from RDC analyses demonstrated that the averaged ensemble structure of $\Delta 131\Delta$ persists largely intact under these same denaturing conditions (Ackerman and Shortle 2002b). Thus, the structural interpretation of relaxation studies of denatured proteins must be less straightforward than for folded proteins.

Discussion

All three ^{15}N relaxation parameters used to characterize the change in dynamics of $\Delta 131\Delta$ produced by low pH, 8 M urea, or multiple hydrophobic substitutions report significant increases in fast dynamic motions. In contrast, effects of these denaturing conditions on global structure reported by RDCs are surprisingly small (Shortle and Ackerman 2001; Ackerman and Shortle 2002b). The transverse relaxation rate R_2 is the most sensitive indicator of structure, typically manifest as peaks of increased R_2 for chain segments undergoing one of two types of motional slowing: (1) Slower local tumbling or bond-vector reorientation on a time scale shorter than global rotation (i.e., less than 1–10 nsec); (2) chemical exchange R_{ex} , namely very slow (i.e., 100 μsec to 10 msec) interconversion between two or more conformations that are sufficiently long lived (1 msec) to have different, nonaveraged chemical shifts. A previous study of ^{15}N R_2 values of $\Delta 131\Delta$ by application of the standard CPMG method suggested only minor contributions of R_{ex} to these characteristic peaks (Alexandrescu and Shortle 1994), a conclusion supported by a finding of similar values of R_2 at 500 MHz for all residues except those from 94 to 101 (supplemental material). Thus, we attribute most of the increase in R_2 manifest as peaks in ^{15}N relaxation profiles to locally slowed crankshaft motions, a conclusion also reached by Baum and colleagues in their studies of the pro-peptide of subtilisin (Buevich and Baum 1999; Buevich et al. 2001).

This conclusion is at odds with previous interpretations of the effects of mutations on ^{15}N relaxation (e.g., Sinclair and Shortle 1999; Klein-Seetharaman 2002). In these studies, the presence of long-range structure in denatured states was inferred from slowed local motions that were eliminated by changes in amino acid sequence. Although RDC data does not support the loss of significant amounts of long-range structure in mutants of $\Delta 131\Delta$, it must be mentioned that the physical basis of this NMR parameter in denatured proteins is still something of a mystery (Ackerman and Shortle 2002a,b). A detailed, quantitative picture of the structural and dynamic changes that accompany mutations must await a more complete understanding of how ensembles of rapidly interconverting conformations yield time-averaged dipolar couplings. Nevertheless, all evidence to date suggests the magnitude of changes in dipolar couplings in denatured proteins parallels the magnitude of changes in long-range structure (Shortle and Ackerman 2001; Ackerman and Shortle 2002a,b).

As can be seen in Figure 2, lowering the pH from 5.2 to 3.0 leads to a reduction in all three ^{15}N relaxation profiles, a result of enhanced fast motions along the entire chain. Yet the characteristic peaks in R_2 and relaxation interference are still evident. Because further changes were not observed upon lowering the pH to 1.2, simple protonation of side

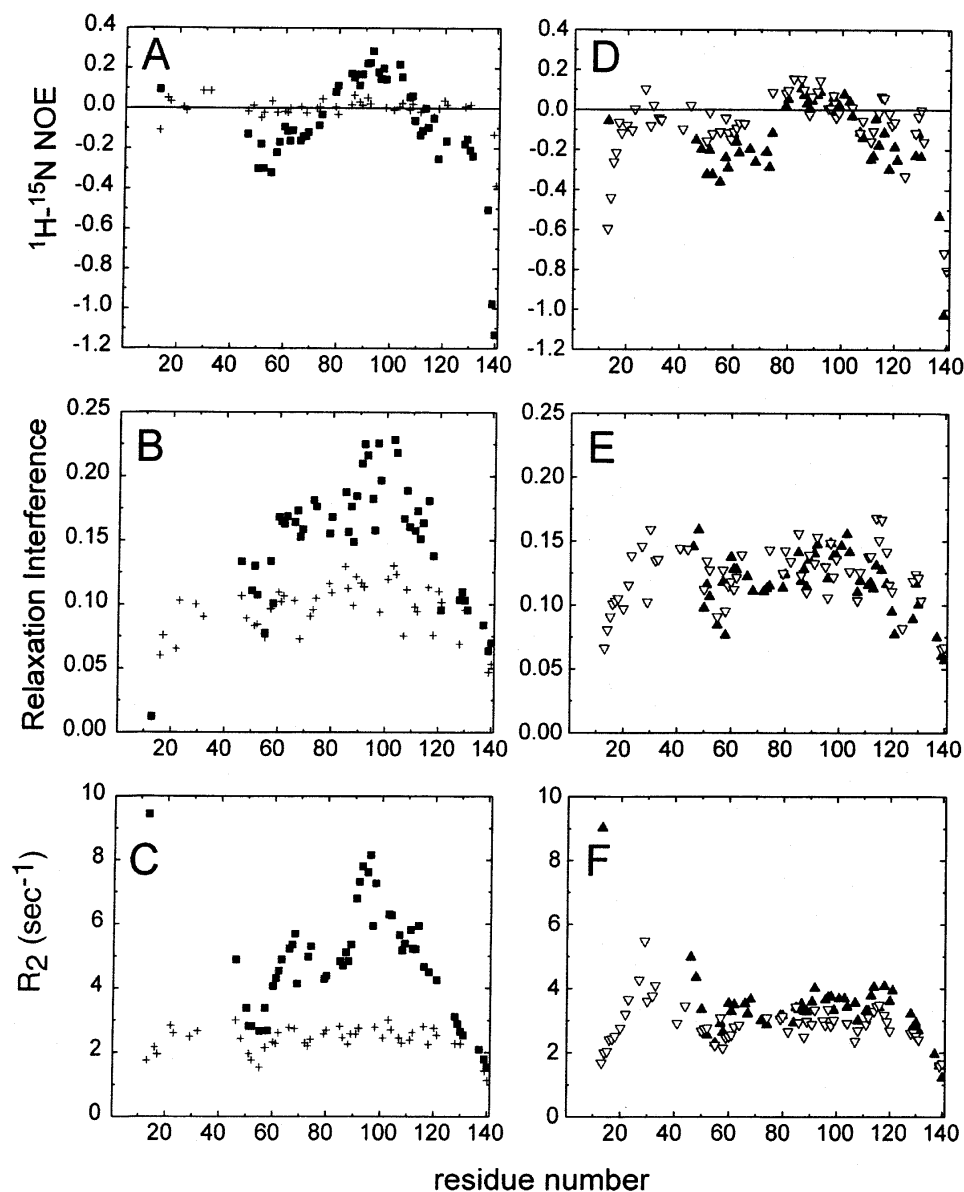


Figure 4. ^{15}N Relaxation profiles of $\Delta 131\Delta$ at pH 5.2 with polar modifications of hydrophobic side chains. *Top (A, D), middle (B, E), and bottom (C, F)* show ^{15}N NOE, relaxation interference, and transverse R_2 profiles, respectively. *Left column (A–C)* shows comparison of the dynamics profiles between $\Delta 131\Delta$ (squares) and the oxo-sextuple mutant (plus signs) at pH 5.2. *Right column (D–F)* shows comparison of the dynamics profiles of the sextuple mutant at pH 5.2 in the absence (solid triangles) and presence (open triangles) of 8 M urea.

chain carboxyl groups (10 glutamates and 6 aspartates in $\Delta 131\Delta$) is probably responsible for these changes in the relaxation profiles. It is noteworthy that this reduction in pH leads to almost no change in the global structure reported by RDCs, with sets of couplings collected at these two values of pH showing a very strong correlation of $r = 0.98$ (Table 1). Consequently, the motional slowing caused by deprotonated carboxy groups must be very local. One possible mechanism is local side-chain/side-chain interactions, through salt bridges with lysines, histidines, and/or ar-

ginines, or through charged hydrogen bonds. A second possibility is that the charged side chains of aspartates and glutamates resist rapid local motions involving coupled variations in their phi/psi angles and rotamer states. A charged, highly hydrated side chain, located close to the polypeptide backbone, may resist motions that place it in environments with a lower dielectric constant, conflict with the energetics of the bound shell of water, or disrupt hydrogen bonding with the backbone. The chemical properties of the protonated side chains of aspartate and glutamate, on the

Table 1. Comparison of ^{15}N relaxation parameters, residual dipolar couplings, and Stokes radius for $\Delta 131\Delta$ without versus with a denaturing perturbation (left column)

	r (NOE)	r (relaxation interference)	r (R_2)	r (RDC)	$r_g/r_g^{\Delta 131\Delta, \text{pH } 5.2}$
Acid (pH 3.0)	0.98	0.92	0.94	0.98 ^a	n.a.
Urea (8 M)	0.80	0.81	0.53	0.82 ^b	1.17 ^b
Sextuple	0.98	0.88	0.74	0.94 ^b	1.05 ^b
Sextuple + urea	0.78	0.74	0.33	0.79 ^b	1.18 ^b
Oxo-sextuple	0.73	0.83	0.53	0.92 ^b	1.08 ^b

^a M.S. Ackerman and D. Shortle, unpubl.

^b Data are taken from Ackerman and Shortle (2002b).

r is the Pearson correlation coefficient between the two data sets. r_g is the Stokes radius.

other hand, should approximate those of asparagine and glutamine.

As seen in Figure 3, the dynamic changes produced by 8 M urea are more diverse and more difficult to explain. The effect on the R_2 profile is larger than that produced by pH 3.0, the characteristic peaks having been eliminated. A new peak appears near the amino terminus, due to breakdown of the beta meander, causing it to become visible in

the NMR spectrum (Wang and Shortle 1995). Because all three peaks (residues 60–75, 85–115, and 25–35) involve chain segments that are more hydrophobic than average (Fig. 5), it seems reasonable to conclude that urea's action of weakening hydrophobic interactions is responsible for these changes in chain dynamics. On the other hand, the NOE profile is elevated except for a segment corresponding to the large R_2 peak (residues 90–105), suggesting most of the chain undergoes a reduction in fast motions. Changes in the relaxation interference profile are intermediate between these two extremes. Control experiments with ethylene glycol suggest the principal mechanism for the more positive NOEs is the 1.7-fold increase in viscosity on addition of 8 M urea. Because the NOE is especially sensitive to very fast subnanosecond motions whereas R_2 is most sensitive to loss of slower motions, we believe the data support an increase in nanosecond motions for the hydrophobic chain segments of the characteristic peaks that is partially concealed by a modest decrease in still faster motions.

Not surprisingly, 8 M urea also has large effects on the global structure of $\Delta 131\Delta$, with the increase in Stokes radius implying that the chain now occupies a volume 60% greater than that in 0 M urea (Table 1). In addition, the change in global structure reported by RDCs is among the

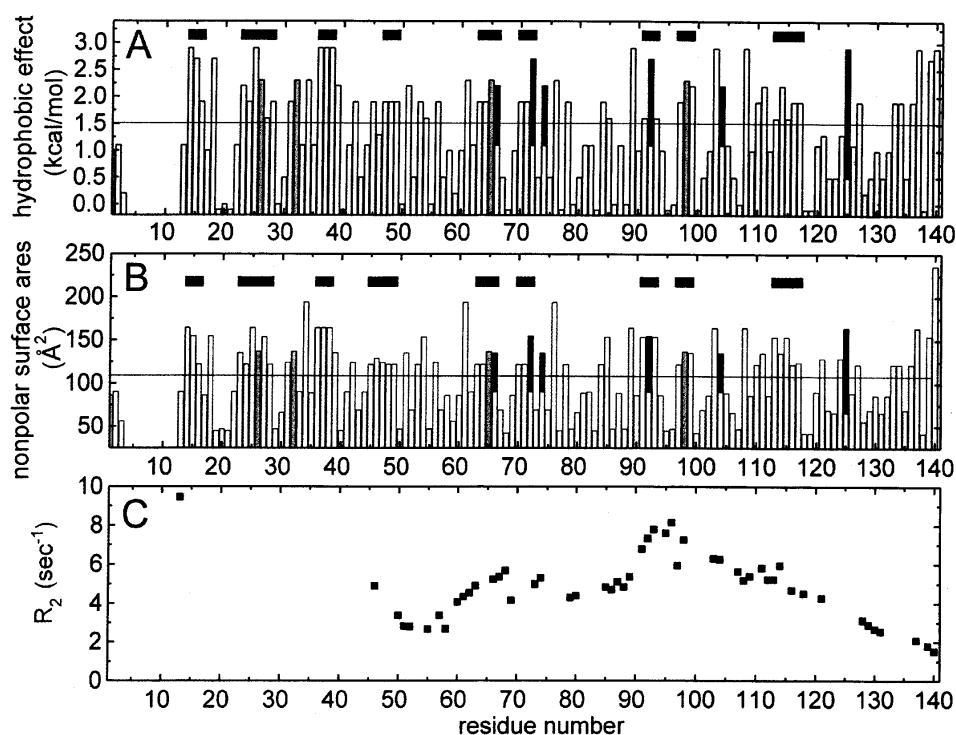


Figure 5. Hydrophobicity scale (A) and nonpolar surface area of side chains (B) of $\Delta 131\Delta$ obtained based on Karplus's values (1997), and the transverse R_2 profile of $\Delta 131\Delta$ at pH 5.2 (C). The straight horizontal lines in (A) and (B) are thresholds for "hydrophobic" made by taking the average of the values for Ala and Val. Segments consisting of more than three consecutive residues with higher values than these thresholds were marked with horizontal bars in (A) and (B). Black vertical bars represent reduced hydrophobicity and nonpolar surface upon the sextuple mutation and gray bars represent methionines that are oxidized in the oxo-sextuple mutant.

largest seen, with the correlation coefficient between sets of couplings dropping to 0.8. Because the urea-induced structural change appears to be larger than that at pH 3.0, the mechanism by which hydrophobic interactions slow chain dynamics could involve longer range interactions. Consequently, it is reasonable to conclude that side-chain/side-chain interactions between hydrophobic residues are responsible to the slower motions reflected in the ^{15}N relaxation profiles of $\Delta 131\Delta$ in buffer.

The combination of 8 M urea and pH 3.0 produces even larger changes in the relaxation profiles (Fig. 3). The R_2 profile is now essentially flat, with no obvious features remaining. The changes in relaxation interference and NOEs are not as dramatic, but in both cases the trend in the data is toward a flat, featureless profile. The fact that lowering the pH further alters ^{15}N relaxation indicates urea by itself does not significantly affect the motional slowing caused by deprotonated carboxyl side chains, even though the polypeptide chain has undergone a large expansion. This finding further supports the proposal that charged aspartates and glutamates act by a very local mechanism and points to some degree of independence between mechanisms by which hydrophobic and acid residues can alter polypeptide chain dynamics.

The effects of multiple hydrophobic substitutions on backbone dynamics were the most dramatic of all. Characteristic peaks in the three relaxation profiles are eliminated, giving essentially flat profiles for both NOEs and R_2 . Presumably these same or similar profiles might arise in 8 M urea if there was no increase in viscosity produced by this solvent. Unlike $\Delta 131\Delta$ in 8 M urea, however, the changes in global structure caused by the 10 substitutions of hydrophobic with polar side chains are relatively modest. From the small increase in Stokes radius, the increase in chain distribution volume is expected to be approximately 25%, while the RDCs remain well correlated with those from unmodified $\Delta 131\Delta$, $r = 0.92$ (Table 1). These more modest changes in global structure suggest the hydrophobic interactions responsible for slower motions may not be long range, but instead may involve contacts between residues relatively nearby in sequence.

When a polypeptide sequence has a local cluster of hydrophobic residues, dynamic motion of the backbone may occasionally be restricted through transient contacts between side chains, even in the absence of stable side-chain packing. The two top panels in Figure 5 show measures of side-chain hydrophobicity and nonpolar surface area (Karplus 1997), plotted for each residue of $\Delta 131\Delta$. The average hydrophobicity for a three residue window was calculated, and a threshold definition of "hydrophobic" was set as the average of alanine and valine. Chain segments consisting of more than three consecutive residues with values above this threshold are marked with horizontal bars in Figure 5. Hydrophobic clusters defined in this way show a

general agreement with the positions of the characteristic peaks in the R_2 profile (Fig. 5C). Moreover, the 10 hydrophobic side-chain modifications are predicted to disrupt each of these local hydrophobic clusters. Thus, the effect of hydrophobic interactions on backbone dynamics may be primarily mediated by local contacts rather than long-range interactions, as proposed by Klein-Seetharaman et al. (2002).

In contrast to the transverse relaxation rate R_2 , the values of the ^1H - ^{15}N steady-state NOE are relatively insensitive to denaturing conditions. The data set for the oxidized-sex-tuple mutant of $\Delta 131\Delta$ show the poorest correlation with the data set for $\Delta 131\Delta$ in buffer (Table I). Random noise, however, is considerably larger in the former data set because essentially all NOE values are approximately zero (Fig. 4A), making the true value of this correlation unclear. Except for this one data set, the magnitude of the changes in NOEs, as quantified by the correlation coefficient, correspond quite closely to those for RDCs, a similarity not seen for the other two relaxation parameters. Although this may be a simple coincidence, it could also reflect a fundamental relationship between the local side-chain interactions that dictate the rates of coupled variations in phi/psi angles and the local interactions that contribute significantly to the average spatial positioning of the chain (topology) in this expanded ensemble of conformations.

The quantitative features of ^{15}N spin relaxation reflect the detailed dynamics of individual HN bond vectors, involving highly local as well as longer range factors. Thus, from first principles it is obvious that interpretation of the structural significance of nonuniform chain dynamics reflected in ^{15}N relaxation peaks must always be problematic. For some proteins, such as hen lysozyme, these peaks may in fact arise from long-range interactions (Klein-Seetharaman et al. 2002). However, in the case of staphylococcal nuclease they clearly do not. Instead, the data suggest they reflect local phenomena whose disruption often has little effect on two NMR parameters that provide reliable measures of ensemble-averaged long-range structure. As demonstrated here, interpretation of ^{15}N relaxation profiles on denatured proteins can be done most convincingly when supplemented with structural data.

Materials and methods

All protein samples were expressed in the *Escherichia coli* BL21(DE3) and purified as described previously (Ackerman and Shortle 2002b). NMR measurements were carried out on a Varian Unity Plus 600 spectrometer and a Varian Unity Plus 500 spectrometer at 32°C using approximately 1.2 mM ^{15}N -labeled protein in 20 mM sodium acetate buffer (pH 5.2) containing 10% $^2\text{H}_2\text{O}$. A microcell tube (Shigemi) was employed for all measurements. The ^1H and ^{15}N frequencies were referenced using amide proton resonances of Ala 112 of $\Delta 131\Delta$ as 8.23 ppm and 127.51 ppm on each ^1H - ^{15}N HSQC spectrum. All the spectra were recorded with 512

(t_2) and 64 (t_1) complex points and spectral widths of 10.0 ppm (^1H) and 23.3 ppm (^{15}N). Steady-state ^1H - ^{15}N NOE measurements were performed using the pulse sequence of Kay with a 3-sec saturation period with additional 3-sec recycle delay. Relaxation interference between ^1H and ^{15}N dipolar coupling and ^{15}N chemical shift anisotropy was measured using the pulse sequence of Tjandra et al. (1996) with a 70-msec delay during the dephasing period. ^{15}N T_2 data were collected using the pulse sequence of Kay (Kay et al. 1992) with a 0.5-msec delay between CPMG refocusing pulses and relaxation times of 10, 30, 50, 70, 90, 110, 130, 150, 170, 190, and 210 msec in an unsorted order to exclude a systematic artifact. Repeated measurements showed an estimate of error around 3% in the signal intensity readings. The decay curve for each residue was analyzed using NMRView (Johnson and Blevins 1994) and errors in the curve fitting were within 3%. Errors in the ^1H - ^{15}N NOE and relaxation interference experiments were estimated based on S/N ratio as described previously (Farrow et al. 1994). In general, the estimates of errors were not much different between the samples except for the $\Delta 131\Delta$ sample at pH 3.0 with 8 M urea and oxo-sextuple $\Delta 131\Delta$, which showed approximately three times larger error due to lower signal level compared to others. Otherwise, for residues near the N and C termini, the estimate of errors was smaller than twice the height of symbols used in Figures 2, 3, and 4. For residues in the more restricted regions, the error estimate is about two–three times the symbol height.

Acknowledgments

We thank M. Ackerman for providing the *E. coli* strain of sextuple $\Delta 131\Delta$ and helpful discussion, K. Dutta for advice on NMR measurements and analysis and for critical manuscript reading, and K. Plaxco for helpful discussions. This work was supported by NIH Grant GM34171 to D.S.

The publication costs of this article were defrayed in part by payment of page charges. This article must therefore be hereby marked “advertisement” in accordance with 18 USC section 1734 solely to indicate this fact.

References

- Ackerman, M.S. and Shortle, D. 2002a. Molecular alignment of denatured states of staphylococcal nuclease with strained polyacrylamide gels and surfactant liquid crystalline phases. *Biochemistry* **41**: 3089–3095.
- . 2002b. Robustness of the long-range structure in denatured staphylococcal nuclease to changes in amino acid sequence. *Biochemistry* **41**: 13791–13797.
- Alexandrescu, A.T. and Shortle, D. 1994. Backbone dynamics of a highly disordered 131 residue fragment of staphylococcal nuclease. *J. Mol. Biol.* **242**: 527–546.
- Bax, A. 2003. Weak alignment offers new NMR opportunities to study protein structure and dynamics. *Protein Sci.* **12**: 1–16.
- Buevich, A.V. and Baum, J. 1999. Dynamics of unfolded proteins: Incorporation of distributions of correlation times in the model free analysis of NMR relaxation data. *J. Am. Chem. Soc.* **121**: 8671–8672.
- Buevich, A.V., Shide, U.P., Inouye, M., and Baum, J. 2001. Backbone dynamics of the natively unfolded pro-peptide of subtilisin by heteronuclear NMR relaxation studies. *J. Biomol. NMR* **20**: 233–249.
- Farrow, N.A., Muhandiram, R., Singer, A.U., Pascal, S.M., Kay, C.M., Gish, G., Shoelson, S.E., Pawson, T., Forman-Kay, J.D., and Kay, L.E. 1994. Backbone dynamics of a free and phosphopeptide-complexed Src homology 2 domain studied by ^{15}N NMR relaxation. *Biochemistry* **33**: 5984–6003.
- Farrow, N.A., Zhang, O., Forman-Kay, J.D., and Kay, L.E. 1995. Comparison of the backbone dynamics of a folded and an unfolded SH3 domain existing in equilibrium in aqueous buffer. *Biochemistry* **34**: 868–878.
- . 1997. Characterization of the backbone dynamics of folded and denatured states of an SH3 domain. *Biochemistry* **36**: 2390–2402.
- Gillespie, J.R. and Shortle, D. 1997. Characterization of long-range structure in the denatured state of staphylococcal nuclease. II. Distance restraints from paramagnetic relaxation and calculation of an ensemble of structures. *J. Mol. Biol.* **268**: 170–184.
- Johnson, B.A. and Blevins, R.A. 1994. NMRView: A computer program for the visualization and analysis of NMR data. *J. Biomol. NMR* **4**: 603–614.
- Karplus, P.A. 1997. Hydrophobicity regained. *Protein Sci.* **6**: 1302–1307.
- Kay, L.E., Keifer, P., and Saarinen, T. 1992. Pure absorption gradient enhanced heteronuclear single quantum correlation spectroscopy with improved sensitivity. *J. Am. Chem. Soc.* **114**: 10663–10665.
- Klein-Seetharaman, J., Oikawa, M., Grimshaw, S.B., Wirmer, J., Duchardt, E., Ueda, T., Imoto, T., Smith, L.J., Dobson, C.M., and Schwalbe, H. 2002. Long-range interactions within a nonnative protein. *Science* **295**: 1719–1722.
- Loll, P.J. and Lattman, E.E. 1989. The crystal structure of the ternary complex of staphylococcal nuclease, Ca^{2+} , and the inhibitor pdTp, refined at 1.65 Å. *Proteins* **5**: 183–201.
- Ohnishi, S. and Shortle, D. 2003. Observation of residual dipolar couplings in short peptides. *Proteins* **50**: 546–551.
- Schwalbe, H., Fiebig, K.M., Buck, M., Jones, J.A., Grimshaw, S.B., Spencer, A., Glaser, S.J., Smith, L.J., and Dobson, C.M. 1997. Structural and dynamical properties of a denatured protein. Heteronuclear 3D NMR experiments and theoretical simulations of lysozyme in 8 M urea. *Biochemistry* **36**: 8977–8991.
- Schwarzinger, S., Wright, P.E., and Dyson, H.J. 2002. Molecular hinges in protein folding: The urea-denatured state of apomyoglobin. *Biochemistry* **41**: 12681–12686.
- Shortle, D. and Ackerman, M.S. 2001. Persistence of native-like topology in a denatured protein in 8 M urea. *Science* **293**: 487–489.
- Sinclair, J.F. and Shortle, D. 1999. Analysis of long-range interactions in a model denatured state of staphylococcal nuclease based on correlated changes in backbone dynamics. *Protein Sci.* **8**: 991–1000.
- Tjandra, N., Szabo, A., and Bax, A. 1996. Protein backbone dynamics and ^{15}N chemical shift anisotropy from quantitative measurement of relaxation interference effects. *J. Am. Chem. Soc.* **118**: 6986–6991.
- Tolman, J.R. 2001. Dipolar couplings as a probe of molecular dynamics and structure in solution. *Curr. Opin. Struct. Biol.* **11**: 532–539.
- Wang, Y. and Shortle, D. 1995. The equilibrium folding pathway of staphylococcal nuclease: Identification of the most stable chain–chain interactions by NMR and CD spectroscopy. *Biochemistry* **34**: 15895–15905.
- Whitten, S.T. and Garcia-Moreno, E.B. 2000. pH dependence of stability of staphylococcal nuclease: Evidence of substantial electrostatic interactions in the denatured state. *Biochemistry* **39**: 14292–14304.
- Yao, J., Chung, J., Eliezer, D., Wright, P.E., and Dyson, H.J. 2001. NMR structural and dynamic characterization of the acid-unfolded state of apomyoglobin provides insights into the early events in protein folding. *Biochemistry* **40**: 3561–3571.